2011 American Control Conference
on O'Farrell Street, San Francisco, CA, USA
June 29 - July 01, 2011

Spatially-localized optimal control of transition to turbulence

Rashad Moarref, Binh K. Lieu, and Mihailo R. Jovanović

Abstract— **For the problem of controlling the onset of turbulence in a channel flow, we study the design of localized optimal state-feedback controllers. The actuation is generated by blowing and suction at the walls and we assume that the actuators are placed along a two-dimensional lattice of equally spaced points, and that each actuator uses information from only a limited number of nearby neighbors. We utilize recently developed tools for designing structured optimal feedback gains to reduce variance amplification of velocity fluctuations in the presence of flow disturbances. Our high-fidelity simulations of nonlinear flow dynamics, conducted at low Reynolds numbers, show that this approach can indeed maintain the laminar flow. This is in contrast to the localized strategies obtained by spatial truncation of optimal centralized controllers, which may introduce instability and promote transition even in the situations where the uncontrolled flow stays laminar.**

Index Terms— **Flow control; structured optimal control; transition to turbulence; Navier-Stokes equations; direct numerical simulations.**

I. Introduction

Feedback strategies for control of fluid flows involve individual system components that are capable of sensing, computation, and actuation. Therefore, an important question in design of flow controllers is related to the interconnection structure between these components. A centralized controller yields best performance at the expense of excessive communication and computation. A fully decentralized controller, while advantageous from a communications perspective, may sacrifice performance. A reasonable compromise between these competing approaches is offered by localized strategies where each component exchanges information with a limited number of nearby components.

Early flow control efforts have focused on drag reduction in turbulent flows. These include the opposition control [1] and gradient-based strategies where the optimal control problem is solved over infinitesimal [2], [3] or finite [4] time horizons. During the last decade, the emphasis has shifted to model-based techniques from linear control theory which represent an efficient means for design of optimal flow controllers [5]–[7]. In this paper, we study the problem of controlling the onset of turbulence. Since the early stages of transition are initiated by large flow sensitivity [8]–[11], we formulate an optimal control problem aimed at reducing this sensitivity. For transition control at low Reynolds numbers, this strategy has proven successful in both vibrational sensorless [12], [13] and centralized feedback [14] setups. These references show that, by substantially reducing large flow sensitivity, transition to turbulence can be prevented and even relaminarization of a fully-developed turbulent flow can be achieved.

R. Moarref, B. K. Lieu, and M. R. Jovanović are with the Department of Electrical and Computer Engineering, University of Minnesota, Minneapolis (e-mails: rashad@umn.edu, lieux006@umn.edu, mihailo@umn.edu).

The main difference between the problem addressed here and in [14] is that we consider control designs that are localized in space. Namely, the actuation at a certain location depends only on local flow information. The localized controller is obtained using recently developed tools for optimal design of feedback gains subject to structural constraints [15], [16]. We compare the performance of the localized optimal controller with that of the optimal centralized controller and the controller that is obtained by spatial truncation of the centralized feedback gain. When the actuators use information from only the nearest neighbor components, we demonstrate the danger of enforcing the constraint by spatial truncation. On the other hand, we show that the localized optimal controller achieves performance comparable to that of the optimal centralized controller.

The paper is organized as follows. In Section II, the evolution model for channel flow subject to body force disturbances and boundary actuation is derived. The problem of optimal state-feedback design in the presence of structural constraints is formulated in Section III. In addition, a gradient descent method for solving necessary conditions for optimality is briefly described. In Section IV, the effectiveness of the designed feedback gains for controlling the onset of turbulence is examined by comparing the sensitivity of the controlled flows to flow with no control. Our design is further verified using direct numerical simulations of the nonlinear flow dynamics. We conclude the paper in Section V.

II. Problem formulation

A. Governing equations

We consider an incompressible channel flow, driven by a fixed pressure gradient and subject to a control actuation in the form of blowing and suction along the walls. The evolution of infinitesimal fluctuations around the laminar parabolic profile $U(y)$ is governed by the linearized Navier-Stokes (NS) equations

$$\mathbf{v}_t = -U\,\mathbf{v}_x - U'\,v_2\,\mathbf{i} - \boldsymbol{\nabla} p + (1/R_c)\Delta\mathbf{v} + \mathbf{d},\ 0 = \boldsymbol{\nabla}\cdot\mathbf{v}, \tag{1}$$

where $\mathbf{i}$ denotes the unit vector in the streamwise direction, and $R_c = U_c\,\delta/\nu$ is the Reynolds number defined in terms of the centerline velocity of the parabolic laminar profile U_c and channel half-height δ. The kinematic viscosity is denoted by ν, p is the pressure, the velocity fluctuations are given by $\mathbf{v} = (v_1, v_2, v_3)$, and $\mathbf{d} = (d_1, d_2, d_3)$ represents the body force disturbance. Here, the indices 1, 2, and 3 correspond to x, y, and z coordinates, respectively, $\boldsymbol{\nabla}$ is the gradient, $\Delta = \boldsymbol{\nabla}\cdot\boldsymbol{\nabla}$ is the Laplacian, and $U'(y) = \mathrm{d}U(y)/\mathrm{d}y$. Actuation along the walls imposes the following boundary conditions

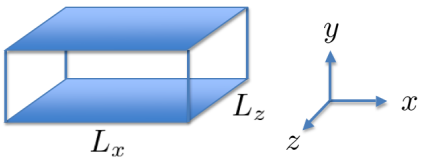

Fig. 1. A periodic channel with size $L_x \times 2 \times L_z$.

on the wall-normal velocity

$$\begin{aligned} v_2(x, y = -1, z, t) &= v_{2,l}(x, z, t), \\ v_2(x, y = 1, z, t) &= v_{2,u}(x, z, t), \end{aligned} \tag{2}$$

where $v_{2,l}$ and $v_{2,u}$ denote actuations at the lower and upper walls. The horizontal velocity components satisfy Dirichlet boundary condition

$$v_1(x, y = \pm 1, z, t) = v_3(x, y = \pm 1, z, t) = 0.$$

To obtain the standard control formulation, the actuation must enter as an explicit input into the evolution equations. The following change of variables

$$\begin{aligned} v_2(x, y, z, t) &= \bar{v}_2(x, y, z, t) + \\ f_l(y)\, v_{2,l}(x, z, t) &+ f_u(y)\, v_{2,u}(x, z, t), \end{aligned} \tag{3}$$

can be used to achieve this objective, where f_l and f_u are specified by the requirement that $\bar{v}_2$ satisfies Dirichlet and Neumann boundary conditions at the walls:

$$f_l(y) = \left(y^3 - 3y + 2\right)/4, \quad f_u(y) = -\left(y^3 - 3y - 2\right)/4.$$

The evolution model for the controlled flow is determined by (see Appendix I for details)

$$\boldsymbol{\phi}_t = \mathcal{A}\,\boldsymbol{\phi} + \mathcal{B}_1\,\mathbf{d} + \mathcal{B}_2\,\mathbf{u}, \quad \mathbf{v} = \mathcal{C}_1\,\boldsymbol{\phi}, \tag{4}$$

where $\boldsymbol{\phi}(x, y, z, t) = \left[\begin{array}{cc} \phi_1^T(x, y, z, t) & \phi_2^T(x, z, t) \end{array}\right]^T$ is the vector of state variables. Here, $\phi_1 = \left[\begin{array}{cc} \bar{v}_2 & \eta \end{array}\right]^T$, where $\eta = v_{1,z} - v_{3,x}$ denotes the wall-normal vorticity, $\phi_2 = \left[\begin{array}{cc} v_{2,l} & v_{2,u} \end{array}\right]^T$ is the boundary-actuation-vector, and $\mathbf{u} = \left[\begin{array}{cc} u_1 & u_2 \end{array}\right]^T = \phi_{2,t}$ is the control input to the evolution model. The operator $\mathcal{A}$ represents the dynamical generator of (4), $\mathcal{B}_1$ and $\mathcal{B}_2$ determine how disturbances and control enter into (4), and $\mathcal{C}_1$ specifies kinematic relation between velocity fluctuations $\mathbf{v}$ and state $\boldsymbol{\phi}$. The definitions of these operators are provided in Appendix I.

B. Actuation along the discrete lattice

In what follows, we impose periodic boundary conditions in the horizontal directions; see Fig. 1 for geometry. The size of the computational domain is given by $L_x \times 2 \times L_z$, where L_x and L_z denote the channel lengths in x and z. We use N_x and N_z Fourier modes to represent differential operators in the streamwise and spanwise directions, respectively. In physical space, this yields a two-dimensional lattice of equally-spaced points $(x_r = rh_x,\, z_s = sh_z)$, with $r \in \mathbb{N}_x = \{0, 1, \ldots, N_x - 1\}$ and $s \in \mathbb{N}_z = \{0, 1, \ldots, N_z - 1\}$. The horizontal spacings between two adjacent points are determined by $h_x = L_x/N_x$ and $h_z = L_z/N_z$. For simplicity, we use the same symbol to denote variables in physical and frequency domains; for example, $v_2(m, n; y, t)$ denotes the frequency representation of $v_2(r, s; y, t) = v_2(x_r, y, z_s, t)$, where $m \in \mathbb{Z}_x = \{-N_x/2, -N_x/2 + 1, \ldots, N_x/2 - 1\}$ and $n \in \mathbb{Z}_z = \{-N_z/2, -N_z/2 + 1, \ldots, N_z/2 - 1\}$. The corresponding spatial wavenumbers are determined by $k_m = m\,2\pi/L_x$ and $k_n = n\,2\pi/L_z$.

We consider the design problem with wall-actuation taking place along the above mentioned two-dimensional lattice. Furthermore, we assume that the states are available for measurement, implying that the control input at (x_r, z_s) is obtained from

$$\begin{aligned} &\mathbf{u}(r, s; t) = \\ &-\sum_{\tilde{r} \in \mathbb{N}_x,\, \tilde{s} \in \mathbb{N}_z} \Big(\int_{-1}^{1} \mathcal{K}_1(r - \tilde{r}, s - \tilde{s}; y)\, \boldsymbol{\phi}_1(\tilde{r}, \tilde{s}; y, t)\, \mathrm{d}y + \\ &\mathcal{K}_2(r - \tilde{r}, s - \tilde{s})\, \boldsymbol{\phi}_2(\tilde{r}, \tilde{s}; t) \Big), \end{aligned} \tag{5}$$

where $\mathcal{K}_1$ and $\mathcal{K}_2$ are the corresponding state-feedback gains. The frequency representation of (5), for each $m \in \mathbb{Z}_x$ and $n \in \mathbb{Z}_z$, is given by

$$\begin{aligned} \mathbf{u}(m, n; t) = &-\int_{-1}^{1} \mathcal{K}_1(m, n; y)\, \boldsymbol{\phi}_1(m, n; y, t)\, \mathrm{d}y - \\ &\mathcal{K}_2(m, n)\, \boldsymbol{\phi}_2(m, n; t). \end{aligned} \tag{6}$$

For computational purposes, the wall-normal operators in (4) and (6) are approximated using pseudospectral method with N_y Chebyshev collocation points [17]. This yields the discretized evolution model

$$\begin{aligned} \dot{\boldsymbol{\phi}}_{m,n} &= A_{m,n}\,\boldsymbol{\phi}_{m,n} + B_{1m,n}\,\mathbf{d}_{m,n} + B_{2m,n}\,\mathbf{u}_{m,n}, \\ \mathbf{v}_{m,n} &= C_{1m,n}\,\boldsymbol{\phi}_{m,n}, \end{aligned} \tag{7}$$

parameterized by $m \in \mathbb{Z}_x$ and $n \in \mathbb{Z}_z$. Here, $\boldsymbol{\phi}_{m,n}(t)$ and $\mathbf{u}_{m,n}(t)$ are column-vectors with $(2N_y + 2)$ and 2 components, respectively, and the dot is the derivative with respect to time. Furthermore, the control action is determined by

$$\mathbf{u}_{m,n} = -K_{m,n}\,\boldsymbol{\phi}_{m,n} = -\left[\begin{array}{cc} K_{1m,n} & K_{2m,n} \end{array}\right] \left[\begin{array}{c} \phi_{1m,n} \\ \phi_{2m,n} \end{array}\right]. \tag{8}$$

where the $2 \times (2N_y + 2)$ matrix $K_{m,n}$ denotes the discretized form of the state-feedback gain in the frequency domain.

III. Design of Localized Optimal Feedback Gains

We consider the problem of designing structured optimal feedback gains for controlling the onset of turbulence. To this end, we determine the stabilizing gains that minimize a performance index J obtained by penalizing flow sensitivity and control effort. These are, respectively, quantified by the variance amplification (i.e., the $\mathcal{H}_2$ norm) of velocity fluctuations $\mathbf{v}$ in the presence of zero-mean white stochastic disturbance $\mathbf{d}$, and by the kinetic energy of the blowing and suction along the walls. In addition, to obtain the well-posed optimal control formulation, the penalty on $\mathbf{u}$ is introduced in the performance index as well.

The above described optimal control problem amounts to finding the stabilizing gains that minimize the variance

amplification of the performance output

$$\boldsymbol{\zeta}_{m,n}(t) = \begin{bmatrix} W^{1/2}\, C_{1m,n} \\ 0 \end{bmatrix} \boldsymbol{\phi}_{m,n}(t) + \begin{bmatrix} 0 \\ R^{1/2} \end{bmatrix} \mathbf{u}_{m,n}(t). \tag{9}$$

Here, R is a positive definite matrix, and W denotes a $3N_y \times 3N_y$ diagonal matrix with $\{\mathbf{w}, \mathbf{w}, \mathbf{w}\}$ on its main diagonal where the vector $\mathbf{w}$ contains the integration weights at the Chebyshev collocation points [18]. Substitution of (8) into (7) and (9) yields the following evolution model of the closed-loop system

$$\begin{aligned} \dot{\boldsymbol{\phi}}_{m,n} &= \left(A_{m,n} - B_{2m,n}\, K_{m,n}\right) \boldsymbol{\phi}_{m,n} + B_{1m,n}\, \mathbf{d}_{m,n}, \\ \boldsymbol{\zeta}_{m,n} &= \begin{bmatrix} W^{1/2}\, C_{1m,n} \\ -R^{1/2}\, K_{m,n} \end{bmatrix} \boldsymbol{\phi}_{m,n}. \end{aligned} \tag{10}$$

Mathematically, the problem of $\mathcal{H}_2$ norm minimization for system (10) can be formulated as [19]

$$\text{minimize}: \quad J(K) = \sum_{m\in\mathbb{Z}_x, n\in\mathbb{Z}_z} \text{trace}\left(X_{m,n}\, Q_{Bm,n}\right), \tag{11a}$$

$$\text{subject to}: \quad A^*_{\text{clm},n}\, X_{m,n} + X_{m,n}\, A_{\text{clm},n} = -\left(Q_{Cm,n} + K^*_{m,n}\, R\, K_{m,n}\right). \tag{11b}$$

Here, * denotes the complex conjugate transpose, $A_{\text{clm},n} = A_{m,n} - B_{2m,n}K_{m,n}$, $Q_{Bm,n} = B_{1m,n}W^{-1}B^*_{1m,n}$, $Q_{Cm,n} = C^*_{1m,n}WC_{1m,n}$, and the solution to (11) in the absence of structural constraints is given by

$$K_{m,n} = R^{-1}\, B^*_{2m,n}\, X_{m,n}, \tag{12}$$

where $X_{m,n}$ is obtained from the algebraic Riccati equation

$$A^*_{m,n}\, X_{m,n} + X_{m,n}\, A_{m,n} + Q_{Cm,n} - X_{m,n}\, B_{2m,n}\, R^{-1}\, B^*_{2m,n}\, X_{m,n} = 0.$$

In general, actuation based on the optimal solution (12) requires knowledge of the complete flow information; namely, the controller is centralized. The problem of designing centralized feedback gains for controlling transition is considered in [14]. As shown by [20], for spatially invariant systems, the magnitude of the centralized feedback gains decays exponentially in space, implying that they can be spatially truncated. Although this suggests one way of obtaining localized controllers, the problem of designing localized optimal feedback gains is more challenging. The fundamental difference between the problem considered here and in [14] is that we ask the following question: *Can actuation based on local flow information prevent transition to turbulence?* To answer this, we a priori impose structural constraints on the feedback gains. It is assumed that each actuator uses information only from the points that are located within a small relative distance. The set of all such relative distances in units of h_x and h_z is denoted by S. In other words, only the feedback gains that correspond to the points in S are allowed to be nonzero. For example, when information from only the nearest neighbors is used, we have (see Fig. 2 for an illustration)

$$S = \left\{(r,s) \;\middle|\; r = \{-1,0,1\}, \quad s = \{-1,0,1\}\right\}.$$

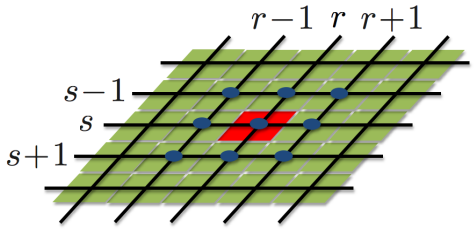

Fig. 2. Sketch of a localized control strategy where the actuator placed at (r, s) uses information from only the nearest neighbors on the lattice.

Furthermore, by $F(r, s)$ we denote the corresponding structured feedback gains.

For spatially invariant systems, the structured optimal state-feedback problem can be formulated as [15]

$$\text{minimize}: \quad J(F) = \sum_{m\in\mathbb{Z}_x, n\in\mathbb{Z}_z} \text{trace}\left(X_{m,n}\, Q_{Bm,n}\right), \tag{P1}$$

$$\text{subject to}: \quad A^*_{\text{clm},n}\, X_{m,n} + X_{m,n}\, A_{\text{clm},n} = -\left(Q_{Cm,n} + C^*_{2m,n}\, F^*\, R\, F\, C_{2m,n}\right). \tag{P2}$$

where F denotes the block-row matrix, that is independent of m and n, and contains the structured feedback gains $F(r, s)$,

$$F = \text{row}\left\{F(r,s)\right\}_{(r,s)\in S}, \tag{P3}$$

and $C_{2m,n}$ is given by the block-column matrix

$$C_{2m,n} = \text{col}\left\{\mathrm{e}^{-\mathrm{i}\,2\pi\,(r\,m/N_x + s\,n/N_z)}\, I\right\}_{(r,s)\in S}. \tag{P4}$$

Here, I is the identity matrix of size $2N_y + 2$, and $A_{\text{clm},n} = A_{m,n} - B_{2m,n}\, F\, C_{2m,n}$ denotes the dynamical generator of the closed-loop system.

Note that in the absence of structural constraints (i.e. $S = \mathbb{N}_x \times \mathbb{N}_z$), the structured optimal control problem (P1)-(P4) reduces to the unstructured problem (11).

A. Computing the structured optimal feedback gains

We briefly describe the method that is employed for solving the optimization problem (P1)-(P4) with specified S. This method is adopted from the development of [15] where efficient descent methods for structured optimal design are introduced.

The necessary conditions for optimality of the stabilizing feedback gain F with $R = rI_{2\times 2}$ in (P2), $r > 0$, are given by [15]

$$\begin{aligned} &A^*_{\text{clm},n}\, X_{m,n} + X_{m,n}\, A_{\text{clm},n} = \\ &\qquad -(Q_{Cm,n} + r\, C^*_{2m,n}\, F^*\, F\, C_{2m,n}), \\ &A_{\text{clm},n}\, Y_{m,n} + Y_{m,n}\, A^*_{\text{clm},n} = -Q_{Bm,n}, \\ &F = \frac{1}{r}\left(\sum_{m\in\mathbb{Z}_x, n\in\mathbb{Z}_z} B^*_{2m,n}\, X_{m,n}\, Y_{m,n}\, C^*_{2m,n}\right) \times \\ &\qquad \left(\sum_{m\in\mathbb{Z}_x, n\in\mathbb{Z}_z} C_{2m,n}\, Y_{m,n}\, C^*_{2m,n}\right)^{-1}. \end{aligned} \tag{14}$$

This system of equations is nonlinear in the unknown matrices $X_{m,n}$, $Y_{m,n}$, and F. Moreover, as seen from the

last condition in Eq. (14), the structural constraints on F introduce coupling between all wavenumbers; this is in contrast to the unstructured optimal control problem given by Eq. (11). Next, we describe the algorithm that is employed for solving (11) [15]:

Descent method for solving (11):

given stabilizing F^0 that satisfies the structural constraints imposed by S,

for $i = 0, 1, 2, \ldots$, **do:**

(1) compute descent direction $\tilde{F}^i$;
(2) determine step-size q^i;
(3) update $F^{i+1} = F^i + q^i \tilde{F}^i$;

until the stopping criterion $||\nabla J(F^i)||_F < \epsilon$ is achieved where $|| \cdot ||_F$ denotes the Frobenius norm and ϵ is the convergence tolerance.

We consider the gradient descent direction that provides linear rate of convergence to the local minimum. More sophisticated descent directions, such as Newton or quasi-Newton directions, provide faster convergence at the expense of increased computational cost. The gradient direction is given by $\tilde{F}^i = -\nabla J(F^i)$ where $\nabla J(F^i)$ is determined from [15]

$$\nabla J(F^i) = \frac{2}{N_x N_z} \sum_{m \in \mathbb{Z}_x, n \in \mathbb{Z}_z} \Big((r\, F\, C_{2m,n} - B^*_{2m,n}\, X_{m,n}) \times Y_{m,n}\, C^*_{2m,n} \Big).$$

For the step-size rule, the backtracking line search [21] is used where in addition to guaranteeing descent of the performance function, we also guarantee the stability of the updated closed-loop system. Namely, we repeat $q^i = \beta q^i$ ($0 < \beta < 1$) until both of the following conditions are satisfied:

(a) descent: $J(F^i + q^i \tilde{F}^i) < J(F^i) + \alpha\, q^i \sum_{m,n} (\nabla J(F^i)^T \tilde{F}^i)$ with $0 < \alpha < 0.5$;
(b) closed-loop stability: $A_{m,n} - B_{2m,n}\, F\, C_{2m,n}$ is stable for all $m \in \mathbb{Z}_x$ and $n \in \mathbb{Z}_z$.

IV. Localized control of transition

As discussed in Section I, the problem of controlling the onset of turbulence is formulated as the $\mathcal{H}_2$ norm reduction problem. Therefore, to assess the effectiveness of feedback controllers, we compare the sensitivity of controlled flows to the sensitivity of flow with no control. We consider the stochastically forced linearized NS equations in the subcritical regime where the flow with no control is linearly stable. The energy density (variance amplification) of fluctuations in the presence of stochastic disturbances is used to quantify the flow sensitivity. The energy density of fluctuations in the presence of stochastic forcing is used to quantify the flow sensitivity. The zero-mean stochastic forcing which is white in time and y, and purely harmonic in horizontal directions, yields a nonzero steady-state variance of velocity fluctuations $E(k_m, k_n)$ [22]. For any $m \in \mathbb{Z}_x$ and $n \in \mathbb{Z}_z$, this quantity can be obtained from

$$\begin{aligned} E(k_m, k_n) &= \text{trace}\,(Z_{m,n}\, Q_{Bm,n}), \\ A^*_{\text{clm},n}\, Z_{m,n} + Z_{m,n}\, A_{\text{clm},n} &= -Q_{Cm,n}. \end{aligned} \tag{15}$$

For the flow with no control (i.e., for $F = 0$), the streamwise-constant fluctuations are the most amplified by the linearized dynamics [10], [11], [22]. These fluctuations correspond to the streamwise streaks that are ubiquitous in wall-bounded shear flows. The large amplification of streaks is physically associated with the vortex-tilting (lift-up) mechanism that arises from the non-normal coupling between dynamics of the wall-normal velocity and vorticity fluctuations [8], [23]. On the other hand, the least stable modes of the uncontrolled flow, i.e., the Tollmien-Schlichting (TS) waves, are much less amplified than the streamwise streaks. This highlights the importance of amplification of the streamwise constant fluctuations in the early stages of transition. Therefore, a control strategy that is capable of reducing the sensitivity of streamwise streaks to stochastic disturbances represents a viable approach for controlling the onset of turbulence.

A. Variance amplification of the controlled flows

For the controlled flows, we consider three state-feedback gains: (a) the centralized gains determined by Eq. (12); (b) the truncated gains obtained by enforcing the structural constraints by spatial truncation of the centralized feedback gains; and (c) the localized optimal gain F that is designed using the method presented in § III-A. For the truncated and localized controllers, we consider the case where each actuator uses information from only its nearest neighbors (for an illustration, see Fig. 2).

Fig. 3 compares the energy amplification of the controlled flows with $R_c = 2000$ and the flow with no control for different horizontal wavenumbers. The optimal centralized controller significantly reduces flow sensitivity for all wavenumbers. Compared with the flow with no control, an 89% reduction in amplification of the most energetic structures (i.e., streaks) is achieved (cf. peak values in Fig. 3(a)).

Next, we look at the flows that are controlled by the truncated centralized and localized feedback gains. Figures 3(b) and 3(c) illustrate that truncated centralized gains introduce instability at small streamwise wavenumbers. The numerical simulations of Section IV-B confirm that the flow controlled with these gains diverges from the laminar mean profile and becomes turbulent. In addition, for the stable wavenumbers, Fig. 3 shows that the variance amplification of the truncated centralized controller is much larger than that of the centralized controller. This justifies the need for designing localized optimal controllers that satisfy the structural constraints and exhibit similar performance to the centralized controller.

Figure 3 shows that the localized optimal gains maintain stability for all wavenumbers. In addition, the variance amplification of the localized controller is similar to that of the centralized controller. In particular, Fig. 3(a) shows that amplification of the most energetic modes is almost the same for localized optimal and centralized controllers. Therefore, the properly designed localized controller is a good candidate for controlling the onset of turbulence, as verified in direct numerical simulations of § IV-B.

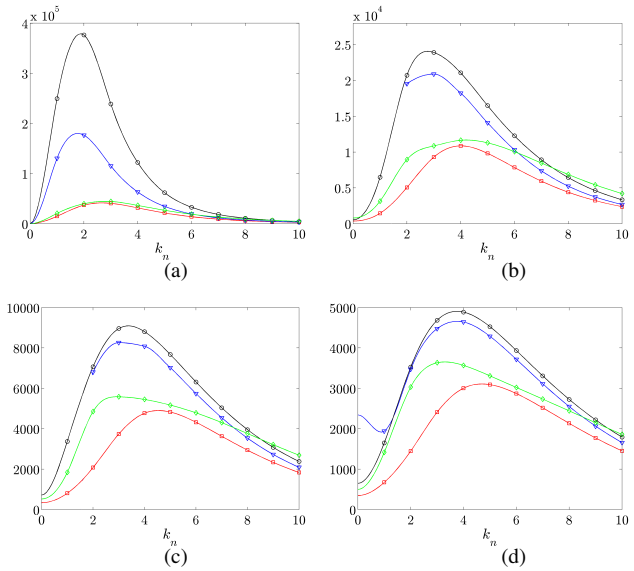

Fig. 3. Variance amplification of the velocity fluctuations $E(k_n)$ for the uncontrolled flow with $R_c = 2000$ ($\circ$) and centralized ($\square$), truncated centralized ($\triangledown$), and localized ($\diamond$) controllers for (a) $k_m = 0$; (b) $k_m = 0.5$; (c) $k_m = 1$; and (d) $k_m = 1.5$. The truncated controller is unstable for $k_m = \{0.5, 1\}$ and $k_n = \{0, 1\}$ and the variance amplification is not defined for these wavenumbers. Note: The variance amplification is computed at the discrete set of wavenumbers k_n and k_m (symbols) and the lines are plotted for visual aid.

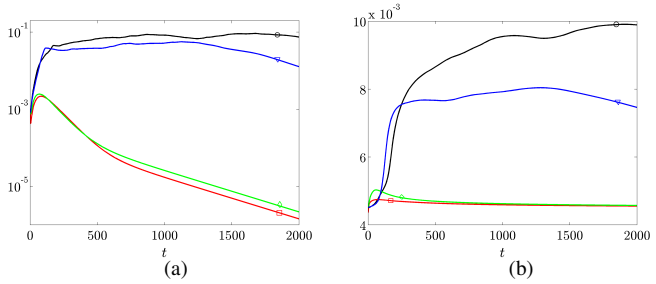

Fig. 4. (a) Energy of the velocity fluctuations $E(t)$; and (b) skin-friction drag coefficient $C_f(t)$ for the flow with no control ($\circ$) and centralized ($\square$), truncated centralized ($\triangledown$), and localized ($\diamond$) controllers. The results are obtained using direct numerical simulations with $R_c = 2000$.

B. Direct numerical simulations

We simulate a channel flow with $R_c = 2000$ that is driven by a constant pressure gradient and is subject to actuation in the form of blowing and suction at the walls. This value of R_c is smaller than the Reynolds number at which linear instability occurs ($R_c = 5772$) and larger than the value for which transition usually takes place in experiments and DNS ($R_c \approx 1000$). The lengths of the computational box in units of the channel half-height δ are $L_x = 4\pi$ and $L_z = 2\pi$, with $N_x \times N_y \times N_z = 52 \times 97 \times 42$ points in x, y, and z directions (after dealiasing in x and z). In our study, 42 collocation points in y were enough for computing convergent feedback gains. These gains are then interpolated and scaled to determine the feedback gains for 97 Chebyshev collocation points.

The flow is initialized with a perturbation that is capable of driving the uncontrolled flow to turbulence. For the optimal centralized, truncated optimal centralized, and localized optimal feedback gains, we evaluate the energy of velocity fluctuations $E(t)$ around the laminar parabolic profile and the skin-friction drag coefficient $C_f(t)$.

Figure 4(a) shows $E(t)$ for the controlled flows and the flow with no control. Compared with its initial value, the energy of three-dimensional fluctuations in the uncontrolled flow is increased by approximately two orders of magnitude, resulting in divergence from the laminar parabolic profile. On the other hand, the optimal centralized controller provides decay of fluctuations' energy to zero after a small transient growth. Our results agree with the study of [14] where it was shown that the optimal centralized controller is capable of preventing transition. The truncated centralized controller introduces faster growth of $E(t)$ relative to the flow with no control, thereby promoting divergence from the laminar flow. On the other hand, Fig. 4(a) shows that the localized optimal controller is capable of maintaining the laminar flow by providing performance comparable to that of the optimal centralized controller.

Figure 4(b) shows the skin-friction drag coefficient $C_f(t)$. We see that the drag coefficients of the optimal centralized and localized controllers are equal to 4.5×10^{-3}, which corresponds to the drag coefficient of the laminar flow. On the other hand, the drag coefficient of the uncontrolled flow is 10^{-2}, which is a clear indicator of a fully developed turbulent flow. The drag coefficient of the truncated centralized controller is approximately 7.5×10^{-3}. This suggests that although the truncated gains cannot maintain the laminar flow, they achieve 16% reduction in drag relative to the uncontrolled turbulent flow.

V. Concluding Remarks

We consider design of localized flow controllers for preventing transition to turbulence. We formulate an optimal control problem for minimizing the flow sensitivity and control effort. In addition, structural constraints are imposed on the feedback gains such that only the gains that are associated with the nearest neighbors are nonzero. This problem is solved using recently developed techniques for designing state-feedback controllers with structural constraints. We show that spatial truncation of the centralized feedback gains can introduce flow instability. Therefore, the truncated feedback gains may not be suitable for controlling transition and they may even promote turbulence in the situations where the uncontrolled flow stays laminar.On the other hand, we demonstrate that the localized optimal controller can exhibit sensitivity reduction similar to that of the optimal centralized controller. Furthermore, our simulations of the nonlinear flow dynamics show that transition can be prevented using localized optimal gains.

Acknowledgments

Part of this work was conducted during the 2010 Center for Turbulence Research Summer Program with financial support from Stanford University and NASA Ames Research Center. We would like to thank Prof. P. Moin for stimulating

discussions and his interest in our work, Dr. J. Larsson for his hospitality during the stay, and Dr. J. W. Nichols for his comments on the early version of this manuscript. Financial support from the National Science Foundation under CAREER Award CMMI-06-44793 is gratefully acknowledged.

APPENDIX I
DETAILS OF THE EVOLUTION MODEL

The evolution model (4) is obtained from the linearized NS equations (1) by eliminating pressure via a standard choice of wall-normal velocity and vorticity (v, η) as the flow variables. By incorporating the change of variables (3) and augmenting the flow variables by the boundary actuations, we obtain the state vector $\boldsymbol{\phi} = \left[\begin{array}{cc} \boldsymbol{\phi}_1^T & \boldsymbol{\phi}_2^T \end{array}\right]^T$, where $\boldsymbol{\phi}_1 = \left[\begin{array}{cc} \bar{v}_2 & \eta \end{array}\right]^T$, and $\boldsymbol{\phi}_2 = \left[\begin{array}{cc} v_{2,l} & v_{2,u} \end{array}\right]^T$. This choice brings the time-derivative of the boundary actuations $\mathbf{u} = \boldsymbol{\phi}_{2,t}$ as an explicit input to the evolution model. The operators in the evolution model are determined by

$$\mathcal{A} = \left[\begin{array}{cc} \mathcal{A}_{11} & \mathcal{A}_{12} \\ 0 & 0 \end{array}\right], \ \mathcal{B}_1 = \left[\begin{array}{c} \mathcal{B}_{11} \\ 0 \end{array}\right], \ \mathcal{B}_2 = \left[\begin{array}{c} \mathcal{B}_{21} \\ \mathcal{B}_{22} \end{array}\right],$$
$$\mathcal{C}_1 = \left[\begin{array}{cc} \mathcal{C}_{11} & \mathcal{C}_{12} \end{array}\right],$$

where

$$\mathcal{A}_{11} = \left[\begin{array}{cc} \Delta^{-1}((1/R_c)\Delta^2 - (U_0\Delta - U_0'')\partial_x) & 0 \\ -U_0'\,\partial_z & (1/R_c)\Delta - U_0\partial_x \end{array}\right],$$

$$\mathcal{A}_{12} = \left[\begin{array}{cc} \mathcal{A}_{12,1} & \mathcal{A}_{12,2} \\ -U_0' f_l\,\partial_z & -U_0' f_u \partial_z \end{array}\right],$$

$$\mathcal{A}_{12,1} = \Delta^{-1}\big((2\,f_l''\,(\partial_x^2+\partial_z^2) + f_l\,(\partial_x^2+\partial_z^2)^2)/R_c - (U_0\,f_l'' + U_0\,f_l\,(\partial_x^2+\partial_z^2) - U_0''\,f_l)\,\partial_x\big),$$

$$\mathcal{A}_{12,2} = \Delta^{-1}\big((2\,f_u''\,(\partial_x^2+\partial_z^2) + f_u\,(\partial_x^2+\partial_z^2)^2)/R_c - (U_0\,f_u'' + U_0\,f_u\,(\partial_x^2+\partial_z^2) - U_0''\,f_u)\,\partial_x\big),$$

$$\mathcal{B}_{11} = \left[\begin{array}{ccc} \Delta^{-1}\,(-\partial_x\partial_y) & \Delta^{-1}\,(\partial_x^2+\partial_z^2) & \Delta^{-1}\,(-\partial_y\partial_z) \\ \partial_z & 0 & -\partial_x \end{array}\right],$$

$$\mathcal{B}_{21} = \left[\begin{array}{cc} \Delta^{-1}\,(-f_l'' - f_l\,(\partial_x^2+\partial_z^2)) & 0 \\ \Delta^{-1}\,(-f_u'' - f_u\,(\partial_x^2+\partial_z^2)) & 0 \end{array}\right]^T,$$

$$\mathcal{B}_{22} = \left[\begin{array}{cc} 1 & 0 \\ 0 & 1 \end{array}\right], \quad \Delta = \partial_x^2 + \partial_y^2 + \partial_z^2,$$

$$\mathcal{C}_{11} = \left[\begin{array}{cc} -\partial_x\partial_y\,(\partial_x^2+\partial_z^2)^{-1} & \partial_z\,(\partial_x^2+\partial_z^2)^{-1} \\ I & 0 \\ -\partial_y\,\partial_z\,(\partial_x^2+\partial_z^2)^{-1} & -\partial_x\,(\partial_x^2+\partial_z^2)^{-1} \end{array}\right],$$

$$\mathcal{C}_{12} = \left[\begin{array}{cc} -f_l'\,\partial_x\,(\partial_x^2+\partial_z^2)^{-1} & -f_u'\,\partial_x\,(\partial_x^2+\partial_z^2)^{-1} \\ f_l & f_u \\ -f_l'\,\partial_z\,(\partial_x^2+\partial_z^2)^{-1} & -f_u'\,\partial_z\,(\partial_x^2+\partial_z^2)^{-1} \end{array}\right].$$

Here, Δ denotes the Laplacian with homogeneous Dirichlet boundary conditions in y and periodic boundary conditions in x and z.

REFERENCES

[1] H. Choi, P. Moin, and J. Kim, "Active turbulence control for drag reduction in wall-bounded flows," *J. Fluid Mech.*, vol. 262, pp. 75–110, 1994.

[2] H. Choi, R. Temam, P. Moin, and J. Kim, "Feedback control for unsteady flow and its application to the stochastic Burgers equation," *J. Fluid Mech.*, vol. 253, pp. 509–543, 1993.

[3] T. Bewley and P. Moin, "Optimal control of turbulent channel flows," *Active Control of Vibration and Noise, ASME-DE*, vol. 75, 1994.

[4] T. Bewley, P. Moin, and R. Temam, "DNS-based predictive control of turbulence: an optimal benchmark for feedback algorithms," *J. Fluid Mech.*, vol. 447, pp. 179–225, 2001.

[5] J. Kim and T. R. Bewley, "A linear systems approach to flow control," *Annu. Rev. Fluid Mech.*, vol. 39, pp. 383–417, 2007.

[6] A. Balogh, W.-J. Liu, and M. Krstić, "Stability enhancement by boundary control in 2D channel flow," *IEEE Trans. Autom. Control*, vol. 46, no. 11, pp. 1696–1711, 2001.

[7] A. Balogh, O. M. Aamo, and M. Krstić, "Optimal Mixing Enhancement in 3-D Pipe Flow," *IEEE Trans. Autom. Control*, vol. 13, no. 1, pp. 27–41, 2005.

[8] K. M. Butler and B. F. Farrell, "Three-dimensional optimal perturbations in viscous shear flow," *Phys. Fluids A*, vol. 4, p. 1637, 1992.

[9] L. N. Trefethen, A. E. Trefethen, S. C. Reddy, and T. A. Driscoll, "Hydrodynamic stability without eigenvalues," *Science*, vol. 261, pp. 578–584, 1993.

[10] B. Bamieh and M. Dahleh, "Energy amplification in channel flows with stochastic excitation," *Phys. Fluids*, vol. 13, no. 11, pp. 3258–3269, 2001.

[11] M. R. Jovanović and B. Bamieh, "Componentwise energy amplification in channel flows," *J. Fluid Mech.*, vol. 534, pp. 145–183, July 2005.

[12] R. Moarref and M. R. Jovanović, "Controlling the onset of turbulence by streamwise traveling waves. Part 1: Receptivity analysis," *J. Fluid Mech.*, vol. 663, pp. 70–99, November 2010.

[13] B. Lieu, R. Moarref, and M. R. Jovanović, "Controlling the onset of turbulence by streamwise traveling waves. Part 2: Direct numerical simulations," *J. Fluid Mech.*, vol. 663, pp. 100–119, November 2010.

[14] M. Högberg, T. R. Bewley, and D. S. Henningson, "Linear feedback control and estimation of transition in plane channel flow," *J. Fluid Mech.*, vol. 481, pp. 149–175, 2003.

[15] M. Fardad, F. Lin, and M. R. Jovanović, "On the optimal design of structured feedback gains for interconnected systems," in *Proceedings of the 48th IEEE Conference on Decision and Control*, Shanghai, China, 2009, pp. 978–983.

[16] F. Lin, M. Fardad, and M. R. Jovanović, "Augmented Lagrangian approach to design of structured optimal state feedback gains," *IEEE Trans. Automat. Control*, 2010, submitted.

[17] J. A. C. Weideman and S. C. Reddy, "A MATLAB differentiation matrix suite," *ACM Transactions on Mathematical Software*, vol. 26, no. 4, pp. 465–519, December 2000.

[18] A. Hanifi, P. Schmid, and D. Henningson, "Transient growth in compressible boundary layer flow," *Phys. Fluids*, vol. 8, no. 3, pp. 826–837, 1996.

[19] K. Zhou, J. C. Doyle, and K. Glover, *Robust and Optimal Control*. Prentice Hall, 1996.

[20] B. Bamieh, F. Paganini, and M. A. Dahleh, "Distributed control of spatially invariant systems," *IEEE Transactions on Automatic Control*, vol. 47, no. 7, pp. 1091–1107, July 2002.

[21] S. Boyd and L. Vandenberghe, *Convex optimization*. New York: Cambridge University Press, 2004.

[22] B. F. Farrell and P. J. Ioannou, "Stochastic forcing of the linearized Navier-Stokes equations," *Phys. Fluids A*, vol. 5, no. 11, pp. 2600–2609, 1993.

[23] S. C. Reddy and D. S. Henningson, "Energy growth in viscous channel flows," *J. Fluid Mech.*, vol. 252, pp. 209–238, 1993.